Articles

A Permanent Hole Burning Study of the FMO Antenna Complex of the Green Sulfur Bacterium *Prosthecochloris aestuarii*†

Eric M. Franken, Sieglinde Neerken, Rob J. W. Louwe, Jan Amesz, and Thijs J. Aartsma*

Department of Biophysics, Leiden University, P.O. Box 9504, 2300 RA Leiden, The Netherlands

Received September 10, 1997; Revised Manuscript Received January 14, 1998

ABSTRACT: A permanent hole burning study on the Fenna−Matthews−Olson, or FMO, antenna complex of the green sulfur bacterium *Prosthecochloris aestuarii* was carried out at 6 K. Excitation resulted not only in relatively sharp features resonant with the burn wavelength but also in broad absorbance changes in the wavelength region of 800−820 nm. The shape of the latter changes was almost independent of the wavelength of excitation. Evidence is given that they are induced by a different mechanism than that which causes the resonant holes and that they may be due to a conformational change of the protein. The original spectrum was restored upon warming to 60 K. The effective dephasing times T_2, as obtained from the homogeneous line widths, increased from about 0.5 ps at 803 nm to ≥20 ps at 830 nm and are in good agreement with recent measurements of accumulated photon-echo and time-resolved absorbance changes.

The Fenna−Matthews−Olson (FMO)[1] complex of green sulfur bacteria, also known as the water-soluble bacteriochlorophyll (BChl) *a* antenna complex, connects the chlorosome, the large antenna structure of these bacteria, to the reaction center complex which is embedded in the membrane. The FMO pigment−protein complex is a trimer, of which each monomer contains 7 BChl *a* molecules.

Since the crystal structure was elucidated in 1975 by Fenna and Matthews (*1*), the FMO complex has been studied extensively by means of various spectroscopic techniques (*2*−*10*), and it has been a subject of theoretical calculations (*11*−*15*). The FMO complex may be considered as an important test case for a theoretical analysis in terms of an exciton model. Until recently (*16*), such an analysis has not been very successful.

There is no full agreement between experimental results from different laboratories. Hole burning, time-resolved absorbance, and accumulated photon-echo (APE) measurements all provide information about the excited-state dynamics of the FMO complex. However, despite the complementary nature of these techniques, the conclusions based on hole burning (*3*) on one hand and APE (*5, 6*) and time-resolved absorbance (*8, 10*) studies on the other are quite different, especially with respect to the wavelength region of 800−815 nm. For this region, Johnson and Small (*3*) reported from hole burning measurements on the FMO complex of *Prosthecochloris aestuarii* a wavelength-independent excited-state lifetime (T_1) of 100 fs at 4.2 K, which they attributed to downward relaxation within the Q_y-manifold of excited states. For longer wavelengths (824−827 nm) a lifetime longer than 20 ps was reported. The lifetimes deduced from APE measurements at the same temperature by Louwe and Aartsma (*5, 7*) increased from sub-picoseconds at 790 nm up to several hundred picoseconds at 830 nm. Especially at intermediate wavelengths, the APE results (e.g., T_2 = 4 ps at 815 nm) deviate considerably from those obtained by hole burning. The time-resolved absorbance measurements performed at 10 K by Vulto et al. (*10*) also indicate excited-state lifetimes that increase with the excitation wavelength used: 0.5, 1.7, 5.5, and 37 ps at 804, 812, 815, and 825 nm, respectively. Similar time constants were obtained by Savikhin and Struve (*8*) for isolated FMO complexes from *Chlorobium tepidum*.

To resolve this apparent contradiction between hole burning and time-resolved absorbance measurements, we reinvestigated the FMO complex using permanent hole burning. Upon hole burning, not only relatively narrow, resonant holes were observed, but also spectrally broad absorbance changes over most of the Q_y absorption bands of FMO, independent of the wavelength of excitation. The assignment of these broad features is a crucial factor in the determination of the excited-state dynamics from the observed absorbance changes. Our data indicate that the narrow holes and the broad absorbance changes are due to two different processes. This leads to an interpretation which deviates fundamentally from the one proposed previously

† Supported by the European Community (Contract FMRX-CT96-0081) and by the Life Sciences Foundation (SLW), which was subsidized by The Netherlands Organization for Scientific Research (NWO).

* To whom correspondence should be addressed. E-mail: aartsma@biophys.leidenuniv.nl. Fax: +31 71 5275819.

[1] Abbreviations: APE, accumulated photon-echo; BChl, bacteriochlorophyll; FMO, Fenna−Matthews−Olson BChl *a* antenna complex; T − S, triplet minus singlet; *P. aestuarii*, *Prosthecochloris aestuarii*.

S0006-2960(97)02264-2 CCC: $15.00
Published on Web 03/26/1998

by Johnson and Small (*3*), who considered the broad absorbance differences to be correlated resonant and nonresonant (satellite) holes, while the relatively sharp zero-phonon holes below 820 nm were considered to be due to secondary hole burning. With our interpretation we obtain good agreement between the hole burning data and the results from APE and transient absorption measurements (*5*−*7*, *10*).

MATERIALS AND METHODS

The green sulfur bacterium *P. aestuarii* was grown in a mixed culture as described by Holt et al. (*17*). The FMO protein was isolated as described by Francke and Amesz (*18*) and dissolved in a 50 mM HCl-Tris buffer at pH 8.3 in the presence of 200 mM NaCl. Glycerol (66%, v/v) was added to obtain a clear glass at low temperatures. The sample was contained in a 1-mm cuvette, with an absorbance at 809 nm of about 0.6 at room temperature. All measurements were performed at 6 K in a helium-flow cryostat (Utreks-LSO, Estonia).

Hole burning was achieved by irradiating the sample during a time t_b at a specific wavelength with the output of a tunable, narrow-bandwidth Nd:YAG-pumped Ti:sapphire laser (Continuum Ti-60; bandwidth, <0.1 cm^{-1}; flash duration, 6 ns), operating at a repetition rate of 10 Hz. Absorption spectra before and after the hole burning procedure were obtained by scanning the wavelength of the Ti:sapphire laser at 0.02−0.15 nm/s. Typical intensities used were 25 mW cm^{-2} for hole burning and 5 nW cm^{-2} for probing the spectra, attained by inserting neutral density filters into the beam. The incident as well as the transmitted laser pulse intensities were recorded, from which the absorbance of the sample was calculated for each laser pulse and then averaged. For detection of the laser pulse intensities, we used two integrating HUV-4000 photodetectors (EG&G), the output of which was sampled and digitized a few microseconds after each flash.

The hole widths in the difference spectra at the burn wavelength were measured as a function of the so-called burn fluence Pt_b/A, with P indicating the average laser power; t_b, the burning time; and A, the cross-sectional area of the laser beam (0.2 cm^2).

RESULTS

The preburn absorption spectrum of the FMO complex measured at 6 K (Figure 1B, dotted line) was in good agreement with the spectra recorded earlier by Whitten et al. (*19*) and Francke and Amesz (*18*). An overview of the absorbance difference spectra as observed upon burning at various wavelengths is presented in Figure 1A. The spectra clearly demonstrate that optical excitation results not only in relatively sharp spectral features resonant with the burn wavelength but also in broad absorbance changes in the region of 800−820 nm, with maxima and minima located around 804, 809, and 814 nm. In contrast to the results of Johnson and Small (*3*), no significant broad-band absorbance differences were observed above 820 nm. The broad absorbance changes were observed both for excitation at 532 nm, i.e., exciting all BChl *a* molecules, and for narrow-banded excitation in the Q_y absorption band of the BChl *a* pigment−protein complex. The shape of the broad features was nearly independent of the excitation wavelength. Upon excitation beyond 823 nm, the amplitude of the broad changes decreased sharply, and they were not observed upon excitation above 827 nm.

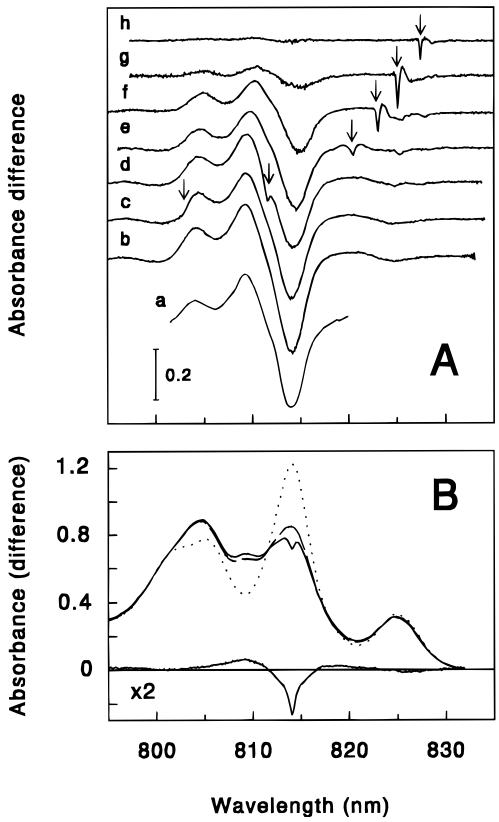

FIGURE 1: (A) Absorption difference spectra at 6 K upon nonspecific excitation at 532 nm (a) and specific excitation at 794 (b), 803 (c), 811.5 (d), 820.5 (e), 823 (f), 825 (g), and 827.5 nm (h). Burn fluences: 1000 (e, g, h), 1600 (c), and 3000 mW min cm^{-2} (b, d, f). The arrows indicate the burn wavelengths. (B) Preburn absorption spectrum (dotted line) and spectrum after burning at 794 nm (burn fluence, 3300 mW min cm^{-2}; dashed line). The solid lines indicate the spectrum after a subsequent burning at 814 nm (burn fluence, 1400 mW min cm^{-2}, adjusted to obtain a zero net absorbance difference over the whole Q_y region) and the resulting absorbance difference.

Both the burned holes and the broad absorbance changes disappeared upon warming. After the temperature of the excited sample had been raised temporarily to 60 K, the absorbance spectrum recorded at 6 K was identical to the preburn spectrum. This indicates that no irreversible photochemistry had occurred, and therefore both features must be the result of reversible photophysical changes. The observation that the net absorbance difference is zero over the whole Q_y region supports this conclusion.

The correlation between the contribution of the narrow holes and that of the broad absorbance differences was investigated further in the following experiment, the results of which are shown in Figure 1B. The sample was burned excessively at the blue side of the Q_y region (at 794 nm), thus creating large changes in the absorbance spectrum (dashed line). Given the homogeneous line width at 794 nm derived from other experiments (*7*, *10*), excitation at this wavelength is nonselective; all FMO complexes were excited. Afterward, the sample was excited at 814 nm, which resulted in a narrow hole at the burn wavelength, having similar characteristics as holes obtained without preburning the sample. However, the broad absorbance changes did not

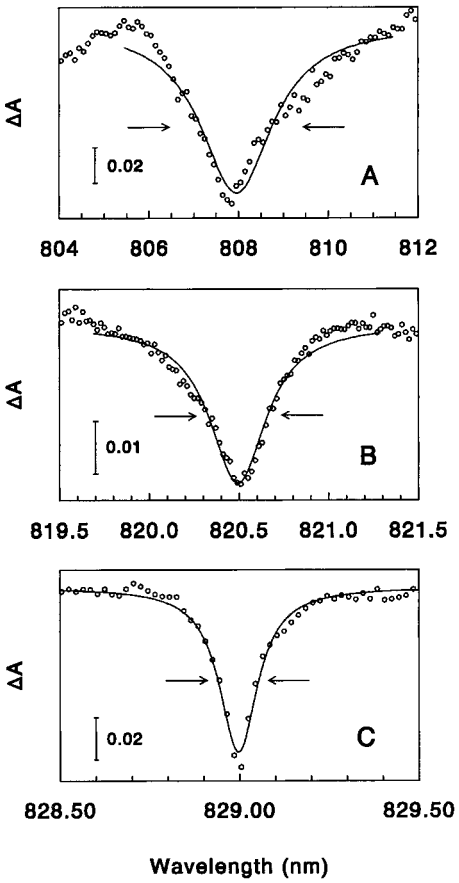

FIGURE 2: Hole burned spectra at 6 K (circles) and corresponding Lorentzian fits upon excitation at 808 (A), 820.5 (B), and 829 nm (C), after burning with 1600 (A) or 1000 mW min cm^{-2} (B, C). Full width at half-maximum of the holes (Γ_{hole}) (see arrows): 1.7 (A), 0.30 (B), and 0.14 nm (C).

increase significantly. Apparently, sharp holes can be obtained at low burn fluence concomitant with the broad absorbance changes, as well as after saturating these broad absorbance changes by excessive burning. This confirms that the sharp holes and the broad absorbance changes are due to different processes. This is corroborated by the fact that the broad spectral changes were independent of the wavelength of excitation and were observed even when the FMO sample was excited at 532 nm. It should also be noted that, upon excitation in the 825 nm band, predominantly sharp holes were observed. Therefore, we conclude that the broad absorbance changes can be treated as uncorrelated background signals, on which the relatively narrow holes are superimposed. Consequently, the hole profiles can be derived from the absorbance difference spectra by subtracting the broad, underlying background signal. For holes burned to the red of 820 nm this subtraction procedure is not necessary, since at these wavelengths no significant background signal is observed (Figure 1A). Some typical hole profiles and corresponding Lorentzian fits upon excitation at different wavelengths are presented in Figure 2.

To account for broadening effects of the observed holes due to saturation and power broadening, the hole widths were measured as a function of the burn fluence and extrapolated to $Pt_b/A = 0$ (*20*). The obtained saturation curves are shown in Figure 3, with Γ_{hole} being the full width at half-maximum of the observed hole and the lines indicating the extrapolations to zero burn fluence. The hole widths increased more

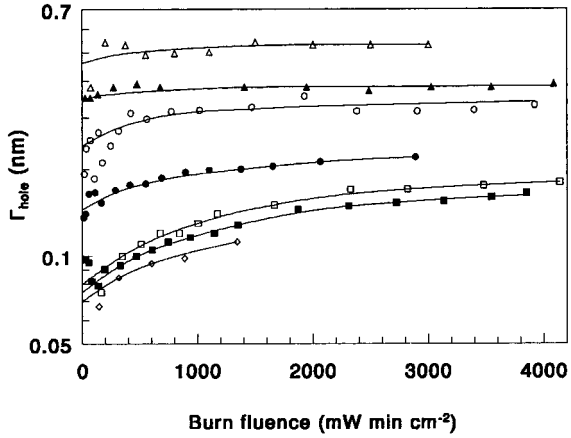

FIGURE 3: Saturation curves of the full width at half-maximum of the holes (Γ_{hole}) upon excitation at 811.5 (△), 817 (▲), 820.5 (○), 823 (●), 826.5 (□), 829 (■), and 830 nm (△). The lines indicate extrapolations to zero burn fluence.

Table 1: Hole Widths (Γ_{hole}) and Corresponding Effective Dephasing Times (T_2) as a Function of Burn Wavelength (λ_{burn})

λ_{burn} (nm)	Γ_{hole} (nm)	Γ_{hole} (cm^{-1})	T_2 (ps)
803	2.7[a]	21[a]	0.5
808	1.7[a]	13[a]	0.8
811.5	0.45	3.4	3.1
817	0.34	2.6	4.2
820.5	0.24	1.8	6.0
823	0.145	1.07	9.9
826.5	0.080[b]	0.59[b]	≥18
829	0.075[b]	0.55[b]	≥19
830	0.070[b]	0.51[b]	≥20

[a] Determined upon burning with 1600 mW min cm^{-2}. [b] Upper limit, because of limited spectral resolution.

or less gradually from 0.07 to 2.7 nm when the burn wavelength was shifted from 830 to 803 nm (Table 1).

The aim of this investigation was to compare information about the excited-state dynamics obtained from hole burning with that based on other spectroscopic techniques. For hole burning, the effective dephasing time T_2 can be calculated from the homogeneous line width (Γ_{hom}) using $\Gamma_{hom} = (\pi T_2)^{-1}$ (*21*). The effective dephasing time T_2 is determined from the excited-state lifetime, T_1, and the pure dephasing time, T_2*, via $(T_2)^{-1} = (2T_1)^{-1} + (T_2^*)^{-1}$. It is reasonable to assume that at 6 K the pure dephasing time T_2* becomes relatively large, and therefore the calculated effective dephasing time is solely determined by the excited-state lifetime T_1. For an inhomogeneously broadened absorption band the observed hole width (Γ_{hole}) is twice the homogeneous line width (*22*).

Table 1 and Figure 4 (solid symbols) show the effective dephasing times derived from the observed holes. The dephasing times at 803 and 808 nm are somewhat less accurate, since the hole widths were determined upon burning with 1600 mW min cm^{-2} and were not extrapolated to zero burn fluence. However, in view of the broad holes produced at these wavelengths, the effect of power and saturation broadening is probably small. The effective dephasing times T_2 display a gradual decrease upon burning at shorter wavelengths from ≥20 ps at 830 nm to about 0.5 ps at 803 nm. Above 825 nm, the derived effective dephasing times may only be a lower limit, because of the limited spectral resolution of our setup.

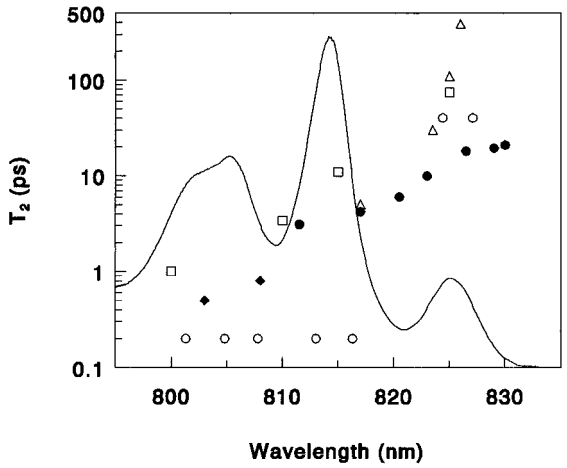

FIGURE 4: Effective dephasing times T_2, derived from hole widths extrapolated to zero burn fluence (●) and from hole widths recorded upon $Pt_b/A = 1600$ mW min cm^{-2} (◆). The open circles represent data reported by Johnson and Small (*3*) based on hole burning measurements at 4.2 K. Results by Louwe and Aartsma (*5, 7*) (APE measurements at 10 K, open triangles) and Vulto et al. (*10*) (pump−probe measurements at 10 K, open squares) are also shown. Solid line: 6 K absorption spectrum.

Apart from the broad background signals and the sharp resonant holes, relatively sharp nonresonant features also could be observed, although their intensity was significantly smaller. Examples of these nonresonant holes are displayed in Figure 5. Trace A shows that, upon burning at 820.5 nm, a nonresonant hole is generated about 5 nm toward lower energies. When the burn wavelength is red-shifted by 1.5 nm from 820.5 to 822 nm (trace B), the nonresonant hole is shifted by the same amount. These observations indicate that the resonant and nonresonant holes are correlated. Trace D indicates that hole burning at 811.5 nm also induces a nonresonant hole around 825 nm. For comparison, trace E is also displayed, which shows the nonresonant hole upon burning at 820 nm. We observed correlated nonresonant holes only at lower energy than the burn wavelength. In particular, excitation at 827.5 nm—in the vicinity of the nonresonant hole induced upon burning at 822 nm—did not generate a nonresonant hole at higher energies (trace C).

DISCUSSION

A key point in the interpretation of the hole burning data is the assignment of the broad absorbance differences that were observed for all excitation wavelengths below 827 nm in addition to the sharp features resonant with the burn wavelength. The shape of these broad absorbance changes is nearly independent of the burn wavelength. The sharp holes were observed in all cases, and they display broadening effects which are typical for hole burning. Moreover, the results shown in Figure 1B indicate that sharp holes are obtained even when the broad absorbance difference signal is saturated. These observations indicate that the broad features are due to a different process than the hole burning mechanism that causes the sharp resonant holes.

The broad background signal may be caused by a migration over the energy landscape of the protein to another local minimum upon excitation (*23*), leading to a change in the absorbance spectrum. Such a process may be induced by the energy deposited in nuclear motion of the pigment−

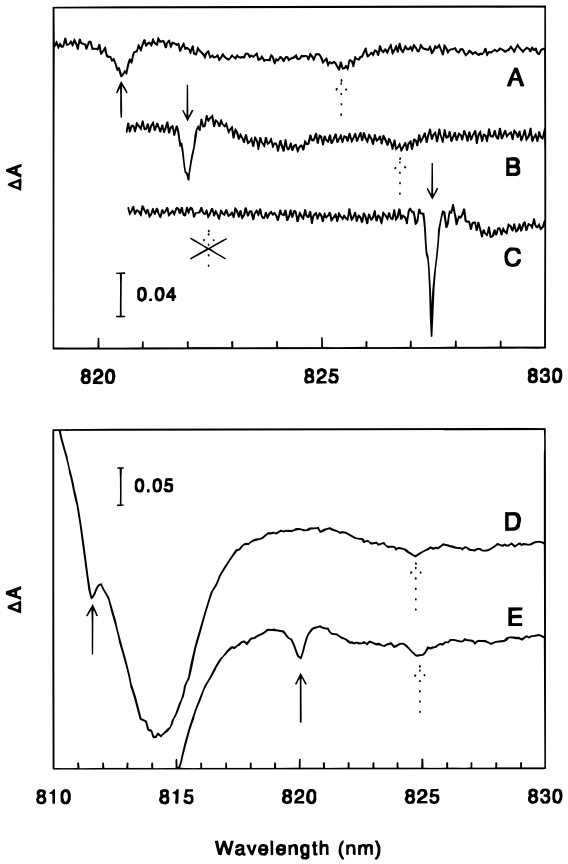

FIGURE 5: Absorbance difference spectra upon burning at 820.5 (A), 822 (B), 827.5 (C), 811.5 (D), and 820 nm (E). Burn fluences: 1000 (A−C) and 3000 mW min cm^{-2} (D, E). The solid arrows indicate the burn wavelengths; the dashed arrows, the nonresonant holes.

protein complex through nonradiative decay to the triplet state or to the ground state. It is preceded by relaxation of the excited-state population to the lowest energy level within the Q_y manifold (*2, 10*), but the energy released by the latter process is presumably much less significant than that of radiationless decay to the triplet and ground states. Since, at 4 K, the latter process always occurs from the same Q_y energy level, the effect of nonradiative decay would be independent of the wavelength of excitation, in agreement with our observations. The excess vibrational energy may be considered as a form of momentary local heating. The decrease of the intensity of the background signal when excitation is to the red of the 825-nm band may be explained by taking into consideration that at these wavelengths only a relatively small subset of all FMO complexes is excited as a result of the relatively narrow homogeneous line widths in this wavelength region. The fact that the 825-nm band is associated with a BChl *a* pigment that does not have significant exciton interactions with the other pigments within a subunit (*16*) may also make this band less susceptible to spectral changes.

The broad absorbance changes are surprisingly large when saturated. It should be kept in mind, however, that the FMO subunit consists of 7 tightly packed BChl *a* molecules in a protein envelope, and a nuclear rearrangement may produce a significant change of the spectrum by affecting multiple pigment molecules. In fact, the difference between the preburn and final absorption spectra is of approximately the same magnitude as that between the absorption spectra of

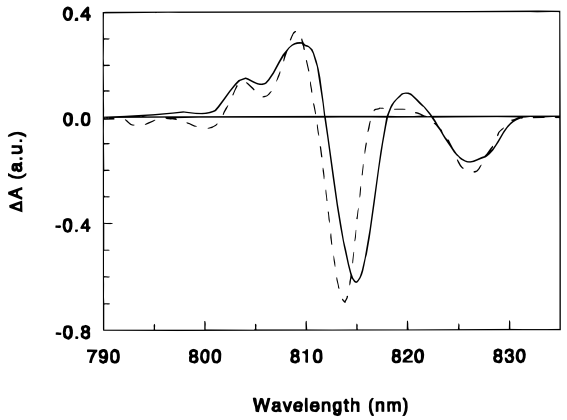

FIGURE 6: Broad absorbance changes observed by Johnson and Small (3) (solid line) and a superposition of the changes observed in this work and the triplet minus singlet absorbance difference spectrum of the FMO complex (*4*, *16*) upon 532-nm excitation at 10 K (dashed line).

the FMO complexes of, for example, *P. aestuarii* and *C. tepidum* (*18*). Broad absorption changes upon prolonged excitation have also been observed in other antenna proteins, of plants as well as of bacteria (*24*−*26*), and it is possible that they have a similar origin as in FMO.

The results of the hole burning experiments presented here can be directly compared to those obtained by Johnson and Small (*3*). As a matter of fact, in most respects the results are similar, especially concerning the sharp resonant holes. Our measurements confirm the weak electron−phonon coupling in this system. There are also significant differences: the broad absorbance change around 825 nm observed by Johnson and Small (*3*) is not reproduced in our measurements, and we also do not observe the features which Johnson and Small (*3*) attribute to satellite holes. A possible explanation for these differences may be given by considering the experimental procedures. We obtained the hole burned spectra by scanning the laser at a much reduced power over the Q_y absorption band, while Johnson and Small (*3*) measured these spectra using a Fourier-transform spectrometer. In the latter case, the light intensity applied to the sample when the spectrum was measured may have been sufficient to accumulate a significant triplet population. Then it is possible that the broad absorbance changes observed by Johnson and Small (*3*) consist of a superposition of the broad absorbance changes observed in our measurements and the triplet minus singlet (T − S) spectrum (*4*, *16*). Indeed, when we perform such a superposition, we can reproduce the general features of the broad absorbance changes observed by Johnson and Small (*3*) (Figure 6). The 825-nm band in the hole burned spectrum of Johnson and Small (*3*) can be accounted for by the bleaching as a result of triplet state formation. The T − S spectrum may also be responsible for at least part of the features which Johnson and Small (*3*) interpreted as satellite holes, but we have not investigated this in more detail.

In clear contrast to the conclusions based on our data, Johnson and Small (*3*) ascribed the large absorbance differences to (non)resonant holes and anti-holes, while they considered the sharp resonant holes below 820 nm as artifacts, due to secondary hole burning. As we already pointed out, our interpretation is fundamentally different. Additional support for our point of view is obtained when we compare the relaxation times given in Table 1 with those measured by other methods. Together with the values from Table 1, we show in Figure 4 the relaxation times obtained by APE measurements (*5*), by time-resolved absorbance experiments (*10*), and from previous hole burning measurements (*3*). Our measured effective dephasing times are in fair agreement with those obtained from APE and time-resolved absorbance measurements and display a gradual increase of the effective dephasing time upon excitation at longer wavelengths. This increase has been attributed to the increased number of relaxation channels that are available after excitation to higher energy levels in the Q_y excited-state manifold of the FMO complex (*5*, *10*).

The interpretation of the large background signals as holes and anti-holes, as used by Johnson and Small (*3*), results in dephasing times of 200 fs from 793.6 to 816.3 nm and ≥40 ps at 824.4 and 827.1 nm, which, at least for the intermediate wavelength region, is much faster than observed by all other methods (Figure 4).

Apart from the broad background signal, relatively sharp nonresonant holes also were observed (see Figure 5). These features contain information on the energy transfer mechanism. The observation of nonresonant holes located to the red side of the burn wavelength confirms the occurrence of excitation transfer to lower energy levels within the Q_y manifold of the FMO complex. However, our data do not reveal any nonresonant holes at higher energies of the burn wavelength, in contrast to the report by Johnson and Small (*3*) in which such features were assigned to the energy levels of individual exciton states in the Q_y band. Although exciton interactions in the FMO complex are significant (*16*), we do not believe that these hole burning data are conclusive, especially in view of the results of recent, much improved simulations of the optical spectra (*16*).

In conclusion, we have presented a new interpretation of the results of hole burning experiments on the FMO complex. The homogeneous line width is determined by rapid relaxation within the Q_y manifold of the FMO complex. The relaxation rates as determined from the homogeneous line width are consistent with those obtained by other methods. We have no indication for correlated nonresonant holes at higher energies of the burn wavelength. Spectrally broad absorbance changes, independent of the excitation wavelength, are indicative of conformational changes in the pigment−protein complex.

ACKNOWLEDGMENT

The authors are indebted to Christof Francke for isolating the FMO complexes.

REFERENCES

1. Fenna, R. E., and Matthews, B. W. (1975) *Nature 258*, 573−577.
2. Swarthoff, T., Amesz, J., Kramer, H. J. M., and Rijgersberg, C. P. (1981) *Isr. J. Chem. 21*, 322−337.
3. Johnson, S. G., and Small, G. J. (1991) *J. Phys. Chem. 95*, 471−479.
4. van Mourik, F., Verwijst, R. R., Mulder, J. M., and van Grondelle, R. (1994) *J. Phys. Chem. 98*, 10307−10312.
5. Louwe, R. J. W., and Aartsma, T. J. (1994) *J. Lumin. 58*, 154−157.

6. Louwe, R. J. W., and Aartsma, T. J. (1995) in *Photosynthesis: From Light to Biosphere* (Mathis, P., Ed.), Vol. I, pp 363−366, Kluwer Academic Publishers, Dordrecht.
7. Louwe, R. J. W., and Aartsma, T. J. (1997) *J. Phys. Chem. B 101*, 7221−7226.
8. Savikhin, S., and Struve, W. S. (1996) *Photosynth. Res. 48*, 271−276.
9. Buck, D. R., Savikhin, S., and Struve, W. S. (1997) *Biophys. J. 72*, 24−36.
10. Vulto, S. I. E., Streltsov, A. M., and Aartsma, T. J. (1997) *J. Phys. Chem. B 101*, 4845−4850.
11. Pearlstein, R. M. (1988) in *Photosynthetic Light Harvesting Systems* (Scheer, H., and Schneider, S., Eds.) pp 555−566, Walter de Gruyter and Co., Berlin.
12. Pearlstein, R. M. (1991) in *Chlorophylls* (Scheer, H., Ed.) pp 1047−1078, CRC press, Boca Raton, FL.
13. Pearlstein, R. M. (1992) *Photosynth. Res. 31*, 213−226.
14. Lu, X., and Pearlstein, R. M. (1993) *Photochem. Photobiol. 57*, 86−91.
15. Gülen, D. (1996) *J. Phys. Chem. 100*, 17683−17689.
16. Louwe, R. J. W., Vrieze, J., Hoff, A. J., and Aartsma, T. J. (1997) *J. Phys. Chem. B 101*, 11200−11207.
17. Holt, S. C., Conti, S. F., and Fuller, R. C. (1966) *J. Bacteriol. 91*, 311−323.
18. Francke, C., and Amesz, J. (1997) *Photosynth. Res. 52*, 137−146.
19. Whitten, W. B., Olson, J. M., and Pearlstein, R. M. (1980) *Biochim. Biophys. Acta 591*, 203−207.
20. Thijssen, H. P. H., and Völker, S. (1985) *Chem. Phys. Lett. 120*, 496−502.
21. Friedrich, J., and Haarer, D. (1984) *Angew. Chem. 96*, 96−123.
22. Friedrich, J. (1995) in *Methods in Enzymology* (Sauer, K., Ed.) Vol. 246, pp 226−259, Academic Press, San Diego.
23. Fritsch, K., Friedrich, J., Parak, F., and Skinner, J. L. (1996) *Proc. Natl. Acad. Sci. U.S.A. 93*, 15141−15145.
24. Chang, H.-C., Jankowiak, R., Yocum, C. F., Picorel, R., Alfonso, M., SM., and Small, G. J. (1994) *J. Phys. Chem. 98*, 7717−7724.
25. Reddy, N. R. S., van Amerongen, H., Kwa, L. S., van Grondelle, R., and Small, G. J. (1994) *J. Phys. Chem. 98*, 4729−4735.
26. Wu, H.-M., Ratsep, M., Lee, I.-J., Cogdell, R. J., and Small, G. J. (1997) *J. Phys. Chem. B101*, 7654−7663.

BI972264C